Available online at www.sciencedirect.com
ScienceDirect
Journal of the European Ceramic Society 28 (2008) 1891–1898
www.elsevier.com/locate/jeurceramsoc

Mechanical properties of hot-pressed ZrB_2–$MoSi_2$–SiC composites

Shu-Qi Guo [a,*], Toshiyuki Nishimura [b], Takashi Mizuguchi [a], Yutaka Kagawa [a,c]

[a] *Composites and Coatings Center, National Institute for Materials Science, 1-2-1 Sengen, Tsukuba, Ibaraki 305-0047, Japan*
[b] *Nano Ceramic Center, National Institute for Materials Science, 1-1 Namiki, Tsukuba, Ibaraki 305-0044, Japan*
[c] *Research Center for Advanced Science and Technology, The University of Tokyo, 4-6-1 Komaba, Meguro-ku, Tokyo 153-8505, Japan*

Received 27 September 2007; received in revised form 17 December 2007; accepted 4 January 2008
Available online 4 March 2008

Abstract

The elastic moduli, hardness, fracture toughness, and flexural strength of a hot-pressed ZrB_2–$MoSi_2$–SiC composite were examined. The effects of $MoSi_2$ and SiC contents were assessed. The dense compacts of ZrB_2–$MoSi_2$–SiC were produced by hot-pressing at 1800 °C for 30 min under a pressure of 30 MPa in vacuum. Ten series compositions of ZrB_2–$MoSi_2$–SiC, with the range from 10 to 40 vol.% for $MoSi_2$ and 5 to 20 vol.% for SiC, were studied. The shear modulus of ZrB_2–$MoSi_2$–SiC was in the range of 190–216 GPa, and Young's modulus measured was in the range of 438–490 GPa. The ranges of hardness and fracture toughness values were measured to be 13.2–16.8 GPa, and 2.6–3.7 MPa $m^{1/2}$, respectively. The average flexural strength of ZrB_2–$MoSi_2$–SiC ranged from 369 to 863 MPa, depending on $MoSi_2$ and SiC contents. The highest strength was obtained for 5 vol.% SiC-containing ZrB_2–$MoSi_2$–SiC, having the value of 863 MPa.

Keywords: ZrB_2–$MoSi_2$–SiC; Elastic moduli; Hardness; Fracture toughness; Flexural strength

1. Introduction

Zirconium diborides (ZrB_2)-based composites have an extremely high melting point (>3000 °C), high thermal and electrical conductivities, chemical inertness against molten metals, and good thermal shock resistance.[1,2] These unique mechanical and physical properties have never been achieved by other ceramics materials. Recently, the ZrB_2-based composites are being considered for use as potential candidates for a variety of high-temperature structural applications, including furnace elements, plasma-arc electrodes, or rocket engines and thermal protection structures for leading-edge parts on hypersonic re-entry space vehicles at over 1800 °C.[3–5] However, the densification of ZrB_2 powder generally requires very high temperatures (>2100 °C) and external pressure because of covalent bond and low self-diffusivity.[6] To improve sinterability, nitrides are added to pure ZrB_2,[7–9] producing an intergranular liquid phase that aids the densification of ZrB_2. In addition, other major problem of ZrB_2-based composites involves high-temperature oxidation.[10,11] To improve oxidation resistance, SiC is added to ZrB_2,[11,12] producing the formation of a protective borosilicate glass at temperature above 1200 °C that enhances oxidation resistance of ZrB_2. Even with these additives, a sintering temperature of above 1900 °C is still required for obtaining near-fully dense ZrB_2-based ceramic composites.

Recently, $MoSi_2$-containing ZrB_2-based composites have been developed. Near-fully dense $MoSi_2$-containing ZrB_2-based composites were sintered by pressureless and/or by hot-press at temperature below 1850 °C.[13,14] Very recently, authors[15] have reported a near-fully dense hot-pressed ZrB_2–$MoSi_2$–SiC composite. The composite showed high thermal and electrical conductivities that depended on compositions. However, the mechanical properties of the ZrB_2–$MoSi_2$–SiC composite and the effects of $MoSi_2$ and SiC contents are not well known. Therefore, it is necessary for the ZrB_2–$MoSi_2$–SiC composites to become familiar with the mechanical properties and correlation to the compositions. In the present study, the ZrB_2-based composites with $MoSi_2$ and/or SiC were hot-pressed at 1800 °C for 30 min under a pressure of 30 MPa in vacuum. The elastic moduli of the composites were calculated using the longitudinal and transverse soundwave velocities measured, whereas the hardness and the fracture toughness of the composites were

* Corresponding author. Tel.: +81 29 859 2223; fax: +81 29 859 2401.
E-mail address: GUO.Shuqi@nims.go.jp (S.-Q. Guo).

0955-2219/$ – see front matter © 2008 Elsevier Ltd. All rights reserved.
doi:10.1016/j.jeurceramsoc.2008.01.003

determined using an indentation crack measurement. The room temperature flexural strength of the composites were determined by fracture using four-point flexural. Also, the effects of $MoSi_2$ and SiC contents on these properties were examined.

2. Experimental procedure

The starting powders used in this study were: ZrB_2 powder (Grade F, Japan New Metals, Tokyo), average particle size ≈2.1 μm, $MoSi_2$ powder (Grade F, Japan New Metals), average particle size ≈3.1 μm; and α-SiC powder (Grade UF-15, H.C. Starck, Berlin, Germany), average particle size ≈0.5 μm. In order to examine the effect of composition on mechanical properties, 10 series of ZrB_2–$MoSi_2$–SiC compositions were prepared in this study. The detailed compositions are shown in Table 1. The powder mixtures were ball-milled in a SiC media using ethanol as a solvent for 24 h and the resulting slurry was then dried. The obtained powder mixtures were hot-pressed (FVHP-1-3, Fuji Electric Co. Ltd., Tokyo, Japan) in the graphite dies at 1800 °C for 30 min under a pressure of 30 MPa in vacuum in tablets averaging 21 mm × 25 mm × 3.5 mm in size. The detailed sintering process has been reported elsewhere.[15] The densities, ρ, of the hot-pressed composite compacts were measured using Archimedes method with distilled water as medium. The theoretical densities of the composites were calculated according to the rule of mixtures. Microstructure of the composites was observed by field emission scanning electron microscopy (FE-SEM). The grain size, d, was determined by measuring the average linear intercept length, d_m, of the grains in FE-SEM images of sintered ZrB_2 ceramics, according to the relationship of $d = 1.56\,d_m$ which was given by Mendenlson.[16]

The elastic moduli measurements of the composites were performed using an ultrasonic equipment (TDS 3052B, Tektronix Inc., Beaverton, OR, USA) with a fundamental frequency of 20 MHz. The shear modulus, G, Young's modulus, E, and Poisson's ratio, ν, were calculated using the longitudinal and transverse soundwave velocities measured in the composite specimens. The detailed calculations were reported elsewhere.[17] On the other hand, the hardness and the fracture toughness, K_{IC}, of the composites were determined using an indentation crack size measurement. The indentation tests were performed on the polished surface of the specimens by loading with a Vickers indenter (AVK-A, Akashi, Co. Ltd., Yokohama, Japan) for 15 s in ambient air at room temperature. The corresponding diagonals of the indentation and crack sizes were measured using an optical microscope attached to the indenter. The indentation load of 98 N was used, and five indents were made for each measurement. The fracture toughness, K_{IC}, of composites were calculated from the Anstis equation.[18] In addition, the ZrB_2–$MoSi_2$–SiC composite plates were cut into a rectangular shape bending test specimen with dimensions of ~25 mm × 2 mm × 2.5 mm for measuring fracture strength. The surfaces of the specimen were ground with a 800-grit diamond wheel and the tensile surface was polished by diamond paste down to 1.0 μm. The edges of the specimen were then chamfered at 45°. The room temperature fracture strength of the composites was determined by fracture, using four-point flexure (inner span 10 mm, outer span 20 mm). The bend test was performed using a testing system (Autograph Model AG-50KNI, Shimadzu Co. Ltd., Kyoto, Japan) with a crosshead speed of 0.5 mm/min. At least five specimens were used for each measurement. After the bend testing, the fracture surfaces of specimens were examined by FE-SEM.

3. Results and discussion

3.1. Densification and microstructure

The measured densities and relative densities of the hot-pressed ZrB_2–$MoSi_2$–SiC composites are summarized in Table 1. From the table, it can be seen that near-fully dense composites to theoretical densities were hot-pressed at 1800 °C under a pressure of 30 MPa with holding time of 30 min for ZrB_2–$MoSi_2$ powder, regardless of $MoSi_2$ amount. This indicated that the addition of $MoSi_2$ significantly improved sinterability of ZrB_2 ceramic and promoted densification of pure ZrB_2 phase at lower temperature. Improvement of densification due to addition of $MoSi_2$ is documented in the literature. Sciti et al.[13] and Bellosi et al.[14] showed that near-fully dense (relative density >98%) ZrB_2-based ceramics with 15 vol.% $MoSi_2$ were obtained by hot-press at 1750 °C under a pressure of 30 MPa with holding time of 45 min, as a result of the presence of intergranular liquid phase. They concluded that the addition of $MoSi_2$ produces an intergranular liquid phase that favors the process of grain rearrangement as well as improves the packing

Table 1
Compositions, densities and relative densities of the hot-pressed ZrB_2–$MoSi_2$–SiC composites

Materials	Compositions (vol.%)			Theoretical density (g/cm^3)	True density (g/cm^3)	Relative density (% TD)
	ZrB_2	$MoSi_2$	SiC			
ZMS-1	90	10	0	6.10	6.08	99.7
ZMS-2	80	20	0	6.12	6.11	99.8
ZMS-3	70	30	0	6.14	6.13	99.8
ZMS-4	60	40	0	6.15	6.13	99.7
ZMS-5	75	20	5	5.98	5.98	100
ZMS-6	70	20	10	5.83	5.79	97.3
ZMS-7	60	20	20	5.55	5.39	94.6
ZMS-8	55	40	5	6.01	6.01	100
ZMS-9	50	40	10	5.86	5.81	99.1
ZMS-10	40	40	20	5.58	5.34	95.7

density of particles, resulting in improved densification. Similar cause is expected for the ZrB_2–$MoSi_2$ materials investigated in this study. On the other hand, the relative densities exceeding 97% were obtained at 1800 °C for the 5 and 10 vol.% SiC-containing ZrB_2–$MoSi_2$–SiC powders. In particular for 5 vol.% SiC, fully dense ZrB_2–$MoSi_2$–SiC compacts were obtained. This suggests that $MoSi_2$ was also sufficient for improving the sinterability of ZrB_2-based composites containing SiC of 10 vol.% or less. For 20 vol.% SiC, however, the density of ~95% was obtained. This means that the densification of ZrB_2–$MoSi_2$–SiC was hindered for 20 vol.% SiC. It is known that the densification behavior depended on the characteristics of intergranular liquid phase formed due to the interactions of the compounds present in the components, including composition, content, viscosity, distribution and wettability. In the present study, the increase of SiC content instead of ZrB_2 means that B_2O_3 reduced while SiO_2 increased. This should be cause the amount of the intergranular liquid phase to decrease and increase the viscosity of the intergranular liquid phase formed which in turn hinders densification. Similar behavior was reported in ZrB_2–SiC–Si_3N_4 composites.[19]

Microstructure of the hot-pressed ZrB_2–$MoSi_2$–SiC composites was observed under backscattered electron FE-SEM imaging, typical examples are shown in Fig. 1. The general

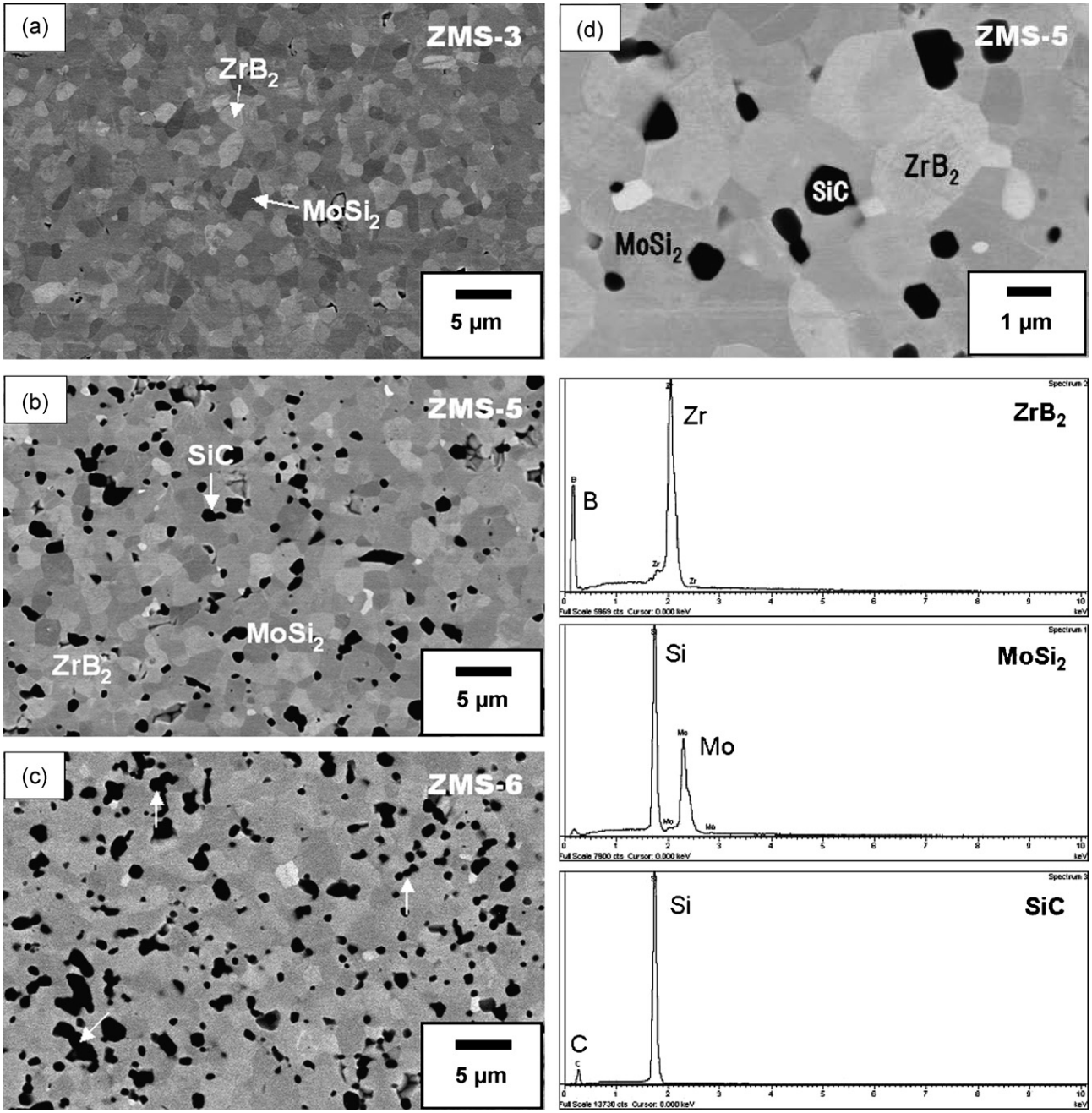

Fig. 1. Typical backscattered electron FE-SEM images of the hot-pressed ZrB_2–$MoSi_2$–SiC composites: (a) ZMS-3, (b) ZMS-5, (c) ZMS-6, and (d) ZMS-5. EDX analysis showed ZrB_2 of light-grey phase, $MoSi_2$ of intermediate-grey phase, and SiC phase with the darkest contrast.

Table 2
Grain sizes of ZrB_2, $MoSi_2$ and SiC measured in the hot-pressed ZrB_2–$MoSi_2$–SiC composites

Materials	Average ZrB_2 grain size (μm)	Maximum ZrB_2 grain size (μm)	Average $MoSi_2$ grain size (μm)	Maximum $MoSi_2$ grain size (μm)	Average SiC grain size (μm)	Maximum SiC grain size (μm)
ZMS-1	1.9 ± 0.6	3.1	1.8 ± 0.5	2.6		
ZMS-2	1.6 ± 0.6	3.4	2.7 ± 0.9	4.3		
ZMS-3	2.1 ± 0.7	3.6	2.4 ± 0.6	3.6		
ZMS-4	1.9 ± 0.7	3.4	2.6 ± 0.8	3.4		
ZMS-5	1.9 ± 0.4	2.6	3.0 ± 0.6	3.9	1.0 ± 0.3	1.4
ZMS-6	2.1 ± 0.9	2.8	3.2 ± 0.6	4.3	1.1 ± 0.9	1.7
ZMS-7	1.9 ± 0.7	2.9	2.1 ± 1.2	4.5	0.8 ± 0.3	1.2
ZMS-8	2.1 ± 0.6	3.2	2.6 ± 0.4	3.1	0.9 ± 0.4	1.5
ZMS-9	3.1 ± 1.1	4.6	4.1 ± 0.6	5.1	1.6 ± 0.8	3.1
ZMS-10	3.8 ± 1.1	5.8	4.0 ± 1.4	6.6	1.9 ± 1.1	4.2

microstructures of the ZrB_2–$MoSi_2$ composites were similar, consisting of the equiaxed ZrB_2 (brighter contrast) and $MoSi_2$ (dark contrast) grains (Fig. 1(a)). For ZrB_2–$MoSi_2$–SiC composition, on the other hand, SiC particles are randomly dispersed among the ZrB_2 and $MoSi_2$ grains boundaries (Fig. 1(b) and (c)). For SiC content of 5 vol.%, SiC particles are almost individually present in the isolated locations (Fig. 1(b)). With increasing SiC content, however, several SiC particles agglomerated to form the small SiC blocks (indicated by arrows in Fig. 1(c)). Under high magnification (Fig. 1(d)), the grain boundaries were clearly seen and the intergranular secondary phase was not observed, at least within the SEM resolution. In addition, EDX analysis identified that the light-grey phase and the intermediate-grey phase in the backscattered electron FE-SEM images are ZrB_2 phase and $MoSi_2$ phase, respectively, and the phase with the darkest contrast is SiC phase.

The grain sizes of ZrB_2, $MoSi_2$, and SiC particles measured in various hot-pressed ZrB_2–$MoSi_2$–SiC composition materials are summarized in Table 2. From this table, the ZrB_2–$MoSi_2$ is found with an average grain size in the range of 1.6–2.1 μm for ZrB_2, and 1.8–2.7 μm for $MoSi_2$. The ranges of the maximum grain size were measured to be 3.1–3.6 and 2.6–4.3 μm for ZrB_2 and $MoSi_2$, respectively. In the case of ZrB_2–$MoSi_2$–SiC, for $MoSi_2$ content of 20 vol.%, SiC addition limited the grain growth of ZrB_2 and slightly affected $MoSi_2$ grain size. For 40 vol.% $MoSi_2$, however, the grain sizes of ZrB_2, $MoSi_2$ and SiC coarsened with SiC content. The major cause of the grains coarsening with SiC is not fully understood but has been closely linked to the intergranular liquid phase formed.

3.2. Elastic properties, hardness and fracture toughness

The shear modulus and Young's modulus of the hot-pressed ZrB_2–$MoSi_2$–SiC composition materials are summarized in Table 3. For ZrB_2–$MoSi_2$ composites, it is found that the shear and Young's moduli decreased with increasing $MoSi_2$ content, however, the two moduli retains a constant between 20 and 30 vol.% $MoSi_2$. For ZrB_2–$MoSi_2$–SiC composites, on the other hand, the shear and Young's moduli remained almost constant for 5 vol.% SiC. This indicated that the addition of 5 vol.% SiC had no effect on the moduli although Young's modulus of SiC phase was lower than that of ZrB_2 phase. With further increasing SiC amount, both the moduli decreased, however. This is associated with the lower moduli of SiC phase as well as with the increase of porosity in ZrB_2–$MoSi_2$–SiC composites (Table 1) because the Young's modulus decreased with increase of pores.[17] Furthermore, the shear and Young's moduli are higher for $MoSi_2$ content of 20 vol.% than for 40 vol.% $MoSi_2$.

The hardness and the fracture toughness of the hot-pressed ZrB_2–$MoSi_2$–SiC composites are also summarized in Table 3. For ZrB_2–$MoSi_2$ composites, the hardness lowered with increasing $MoSi_2$ amount, in particular for $MoSi_2$ content of 40 vol.%, the hardness significantly decreased. These hardness values are comparable with those reported by Sciti et al.[13] and Bellosi et al.[14] in the pressureless and hot-pressed 15 vol.% $MoSi_2$-containing ZrB_2 compacts. However, a low hardness was observed in the 40 vol.% $MoSi_2$-containing ZrB_2 composite due to a large amount of $MoSi_2$. This indicated that the hardness of the composite is dominated by soft $MoSi_2$ phase. In

Table 3
Shear modulus, Young's modulus, Poisson's ratio, hardness, and indentation fracture toughness measured in the hot-pressed ZrB_2–$MoSi_2$–SiC composites

Materials	G (GPa)	E (GPa)	ν	Hardness (GPa)	Fracture toughness (MPa $m^{-1/2}$)
ZMS-1	216 ± 3	490 ± 7	0.14 ± 0.01	15.8 ± 0.7	3.7 ± 0.3
ZMS-2	207 ± 4	472 ± 6	0.14 ± 0.01	16.3 ± 0.9	2.8 ± 0.2
ZMS-3	206 ± 1	473 ± 3	0.15 ± 0.01	15.4 ± 0.7	2.6 ± 0.2
ZMS-4	196 ± 2	448 ± 4	0.14 ± 0.01	13.2 ± 0.7	3.1 ± 0.3
ZMS-5	207 ± 5	476 ± 11	0.15 ± 0.01	16.1 ± 0.5	3.4 ± 0.4
ZMS-6	204 ± 5	465 ± 10	0.14 ± 0.01	16.5 ± 0.5	3.4 ± 0.2
ZMS-7	200 ± 6	461 ± 12	0.15 ± 0.01	16.8 ± 0.9	3.4 ± 0.2
ZMS-8	198 ± 6	450 ± 5	0.14 ± 0.02	14.6 ± 0.5	3.5 ± 0.2
ZMS-9	193 ± 7	442 ± 7	0.15 ± 0.01	15.0 ± 1.0	3.3 ± 0.2
ZMS-10	190 ± 5	438 ± 9	0.15 ± 0.01	16.1 ± 0.5	3.3 ± 0.2

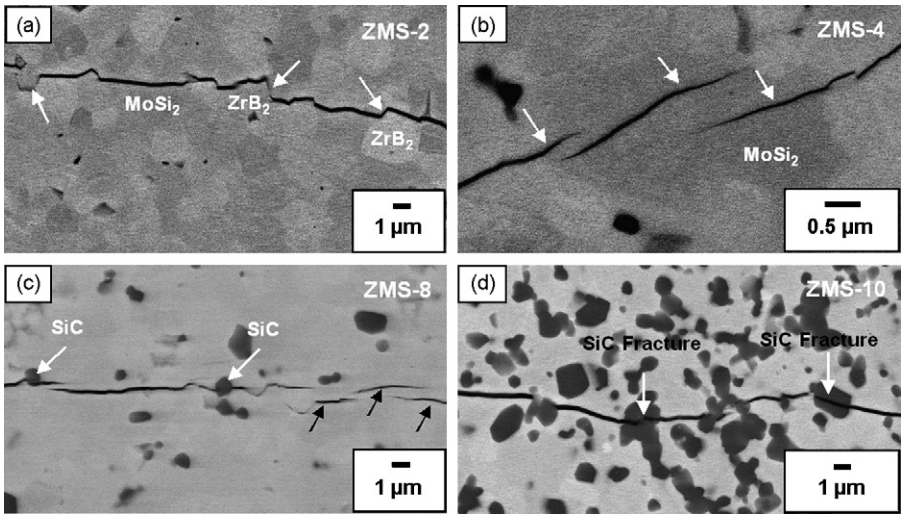

Fig. 2. Typical cracking behavior of the hot-pressed ZrB_2–$MoSi_2$–SiC composites; (a) ZMS-2, (b) ZMS-4, (c) ZMS-8, and (d) ZMS-10.

addition, the fracture toughness decreased with the content of $MoSi_2$. The measured fracture toughness values are comparable with previously reported data of hot-pressed 15 vol.% $MoSi_2$-containing ZrB_2 ceramics.[13,14] One exception is the increase of fracture toughness observed in 40 vol.% $MoSi_2$-containing ZrB_2 composite. Fig. 2 shows the typical SEM micrographs of the indentation cracking behavior of the hot-pressed ZrB_2–$MoSi_2$–SiC composites. The crack propagated along ZrB_2 phase boundaries and across $MoSi_2$ phase in the composites (Fig. 2(a)), respectively, with being deflected along the grain boundaries of ZrB_2, but without being deflected along the grain boundaries of $MoSi_2$ grains. As a result, the fracture toughness decreased with increasing $MoSi_2$ content. However, the multiple cracking behavior was observed in $MoSi_2$ phase for $MoSi_2$ content of 40 vol.% (indicated by arrows in Fig. 2(b)). This is associated with the complex residual stress state that develops during cooling from the pressing temperature due to the thermal expansion mismatch between ZrB_2 and $MoSi_2$. There is a tensile stress in $MoSi_2$ phase, and there is a compressive stress in ZrB_2 phase. The tensile residual stress within $MoSi_2$ grains increased with amount of $MoSi_2$, resulting in turn in multiple cracking. This multiple cracking behavior led to an increase of fracture toughness of ZMS-4 (Table 3), compared with ZMS-2 and ZMS-3.

In the case of ZrB_2–$MoSi_2$–SiC composites, the hardness was almost constant regardless of SiC content for $MoSi_2$ content of 20 vol.%. For 40 vol.% $MoSi_2$, however, the hardness gradually increased with SiC content and the hardness measured was in the range of 13.2–16.1 GPa. On the other hand, the addition of 5 vol.% SiC led to increase of fracture toughness, but the toughness remained nearly the constant even with further increasing SiC content. The detailed observations of cracking behavior exhibited the evidence of crack deflection at SiC grains as well as of multiple cracking for SiC content of 5 vol.% (indicated by arrows in Fig. 2(c)). The crack deflection at SiC grains and the multiple cracking contributed to increase of fracture toughness. However, with higher SiC content, the fracture of larger SiC particles was observed during cracking (indicated by arrows in Fig. 2(d)), but the crack deflection still occurred at the smaller SiC particles. This evidence shows that the fractured larger SiC particles were insufficient for contributing to increase of fracture toughness. The fact of the constant fracture toughness with SiC content suggests that most of the added SiC particles were fractured during cracking for SiC content exceeding 5 vol.%. In addition, only a single crack was observed in the case of higher SiC content instead of multiple cracking for 5 vol.% SiC (Fig. 2(c) and (d)). This cracking behavior could not contribute to increase of fracture toughness of the composites with higher SiC content.

3.3. Flexural strength

In Fig. 3, the room temperature flexural strengths measured in the hot-pressed ZrB_2–$MoSi_2$ composites are presented. From this figure, it is found that the average flexural strength of 10 vol.% $MoSi_2$-containing ZrB_2 ceramic (ZMS-1) was ~800 MPa, and this value is higher than that reported by Bel-

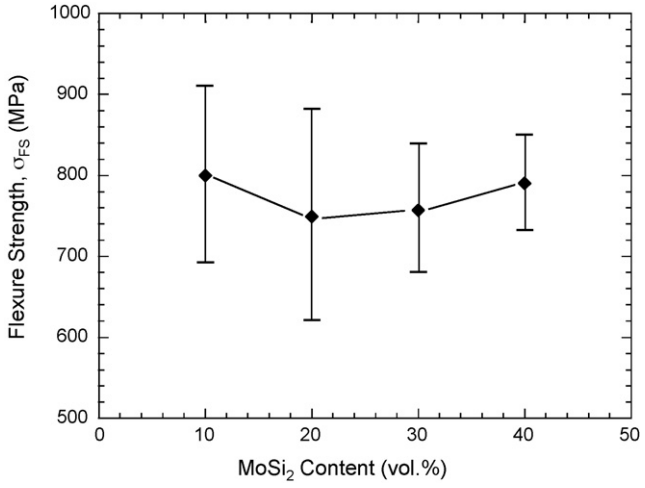

Fig. 3. Plots of flexural strength of the hot-pressed ZrB_2–$MoSi_2$ composites as a function of $MoSi_2$ content.

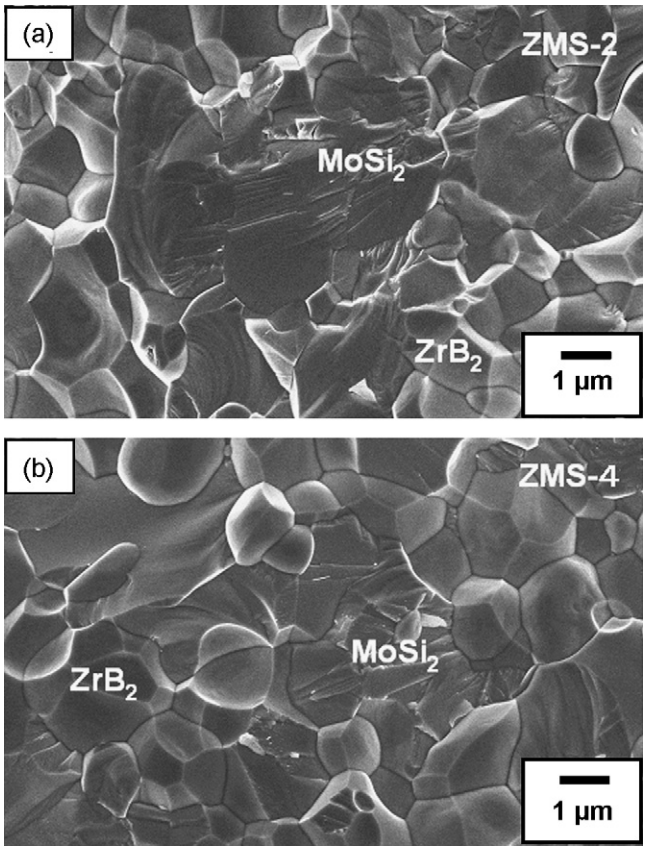

Fig. 4. Typical SEM micrographs of fracture surfaces for the hot-pressed ZrB_2–$MoSi_2$ composites: (a) ZMS-2 and (b) ZMS-4.

losi et al.[14] who showed the strength of hot-pressed 15 vol.% $MoSi_2$-containing ZrB_2 ceramic was ~700 MPa. This difference should be attributed to the presence of more pores because the density of hot-pressed composites reported was 98%,[14] compared to the present materials. The flexural strength lowered then with $MoSi_2$, and subsequently the strength was almost the constant for $MoSi_2$ content ranging from 20 to 30 vol.%. However, the flexural strength increased for 40 vol.% $MoSi_2$ (ZSZ-4). The fracture surface of the ZrB_2–$MoSi_2$ composites was observed under FE-SEM, typical examples are shown in Fig. 4. It is found that the fracture fashion of ZrB_2 phase differed with that of $MoSi_2$ phase: the intergranular fracture for ZrB_2, and intragranular fracture for $MoSi_2$. This fracture characteristic was observed for all the ZrB_2–$MoSi_2$ composites, regardless of $MoSi_2$ content. In addition, some extremely large $MoSi_2$ grains were observed in the fracture surface of ZMS-2 (Fig. 4(a)). These large $MoSi_2$ grains were due to $MoSi_2$ agglomerates. However, the large $MoSi_2$ agglomerates were not observed in the fracture surfaces of ZMS-4 (Fig. 4(b)). An earlier study[13] in a pressureless-sintered ZrB_2–$MoSi_2$ composite showed that the large $MoSi_2$ agglomerates led to the strength loss of the composite. In the present study, it is found that the change in the strength with $MoSi_2$ content is consistent with maximum $MoSi_2$ grain size measured (Table 2). This finding indicated that the strength of ZrB_2–$MoSi_2$ composites is mostly dominated by the maximum $MoSi_2$ grain size in the materials.

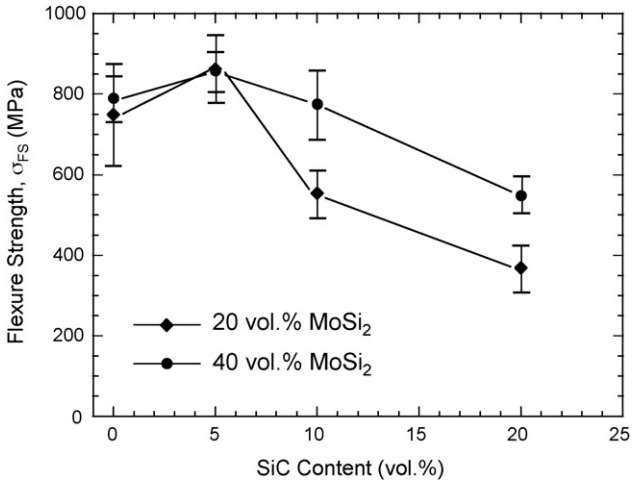

Fig. 5. Plots of flexural strength of the hot-pressed ZrB_2–$MoSi_2$–SiC composites as a function of SiC content.

In Fig. 5, the plots of flexural strength as a function of SiC content for the hot-pressed ZrB_2–$MoSi_2$–SiC composites are presented. It is found that the average flexural strength is the highest for SiC content of 5 vol.%, regardless of $MoSi_2$ content. This high strength is attributed to the fine grains, including ZrB_2, $MoSi_2$ and SiC for this composition material among all the studied materials (Table 2). The flexural strength then lowered with further increasing SiC content. This decrease should be attributed to the presence of more pores (Table 1) as well as to the presence of larger ZrB_2, $MoSi_2$, and SiC particles (Table 2), compared to 5 vol.% SiC. This was consistent with that which was early reported by Rezaie et al.[20] and Zhu et al.[21] in ZrB_2–SiC composites. They showed that the flexural strength of the composite decreased substantially as the average size of SiC grains increased from ~1.2 to 3.1 μm. Zhu et al.[21] also suggests that the largest SiC grains in the microstructure acted as the critical flaws causing the failure of the composite. In addition, the strength loss with SiC addition is larger for $MoSi_2$ content of 20 vol.% than for 40 vol.% $MoSi_2$. This is probably due to more and larger defects for 20 vol.% $MoSi_2$-containing ZrB_2 than 40 vol.%-containing ZrB_2 because a lower relative density for the former than for the latter (Table 1).

The fracture surfaces of the ZrB_2–$MoSi_2$–SiC composites were observed under FE-SEM, typical examples are shown in Fig. 6. It is clearly observed that the fine SiC particles are presented within large $MoSi_2$ phase as well as at the grain boundaries of ZrB_2 and/or $MoSi_2$. This means that the presence of SiC strengthened $MoSi_2$ phase as well as strengthened the grain boundaries of ZrB_2 and/or $MoSi_2$, in turn results in increase of flexural strength of the composites. This strengthening effect is the best for SiC content of 5 vol.% because the fully dense composites, with homogeneously dispersed fine SiC particles, were obtained for both $MoSi_2$ amounts (Table 1 and Fig. 1(b)). For 10 and 20 vol.% SiC, however, the hot-pressed composites are not fully dense. In particular, for $MoSi_2$ content of 20 vol.%, the addition of 10 and 20 vol.% SiC led to significant degradation of sinterability. Some pores were observed in the fracture surfaces of the composites (indicated by arrows in Fig. 6(c) and (d)). The

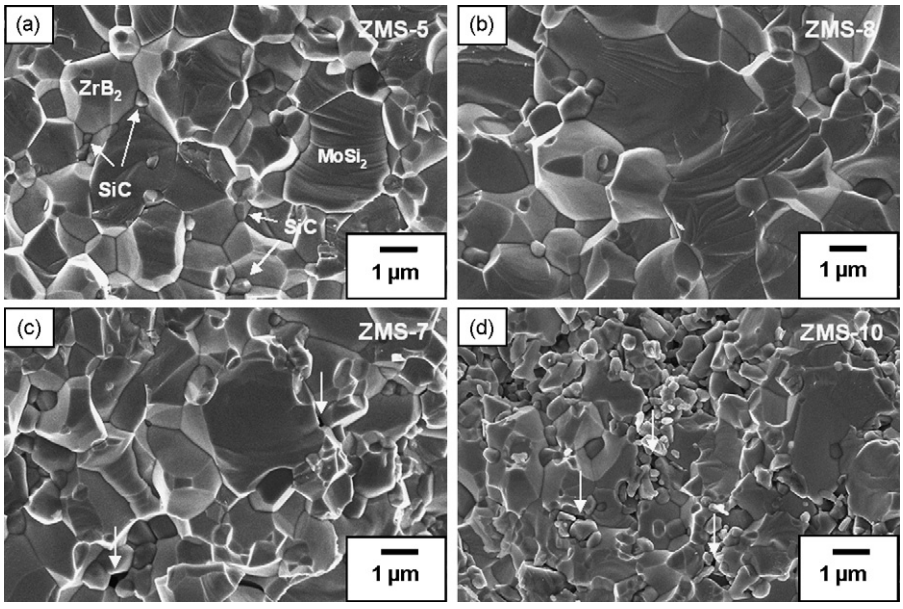

Fig. 6. Typical SEM micrographs of fracture surfaces for the hot-pressed ZrB_2–$MoSi_2$–SiC composites: (a) ZMS-5, (b) ZMS-8, (c) ZMS-7, and (d) ZMS-10.

pores were larger for 20 vol.% $MoSi_2$ than for 40 vol.% $MoSi_2$ (Figs. 6(c) and (d)). The presence of larger pores led to the substantial strength loss of the composites. As a result, although the grains sizes measured were larger for 40 vol.% $MoSi_2$ than for 20 vol.% $MoSi_2$ (Table 2), the loss of flexural strength due to more SiC addition is larger for the latter than for the former.

4. Conclusions

(1) Near-fully dense ZrB_2–$MoSi_2$ composites were hot-pressed at 1800 °C under a pressure of 30 MPa for $MoSi_2$ content ranging from 10 to 40 vol.%. On the other hand, the addition of SiC degraded sinterability of ZrB_2–$MoSi_2$ composites. The relative densities ranging from 94 to 99% were obtained for 10 and 20 vol.% SiC-containing ZrB_2–$MoSi_2$ powders, depending on $MoSi_2$ content.

(2) The shear and Young's moduli of the ZrB_2–$MoSi_2$ composites lowered with $MoSi_2$ content. The addition of 5 vol.% SiC did not decrease the shear and Young's moduli of the ZrB_2–$MoSi_2$–SiC composites, both the moduli decreased with further increasing SiC content, however.

(3) The hardness of ZrB_2–$MoSi_2$ composite decreased with $MoSi_2$ content. In contrast, the hardness of ZrB_2–$MoSi_2$–SiC was almost the constant with SiC content for $MoSi_2$ content of 20 vol.%, but it increased for 40 vol.% $MoSi_2$.

(4) The fracture toughness of ZrB_2–$MoSi_2$ composites decreased with $MoSi_2$ content, but the fracture toughness increased for 40 vol.% $MoSi_2$-containing ZrB_2. Conversely, addition of 5 vol.% SiC led to increase of fracture toughness of ZrB_2–$MoSi_2$–SiC composites, and the toughness was almost constant with further increasing SiC content.

(5) The flexural strength of ZrB_2–$MoSi_2$ composites lowered with $MoSi_2$ content ranging from 10 to 20 vol.%, as a result of large $MoSi_2$ agglomerates. However, the flexural strength of ZrB_2–$MoSi_2$–SiC was the largest for SiC content of 5 vol.%, and the strength then decreased with increasing SiC content. Furthermore, the flexural strength was higher for 40 vol.% $MoSi_2$-containing ZrB_2–SiC than for 20 vol.% $MoSi_2$-containing ZrB_2–SiC.

References

1. Mroz, C., Zirconium diboride. *Am. Ceram. Soc. Bull.*, 1994, **73**(6), 141–142.
2. Telle, R., Sigl, L. S. and Takagi, K., Boride-based hard materials. In *Handbook of Ceramic Hard Materials*, ed. R. Riedel. Wiley–VCH, Wiinheim, Germany, 2000, pp. 803–945.
3. Upadhya, K., Yang, J.-M. and Hoffmann, W. P., Materials for ultrahigh temperature structural applications. *Am. Ceram. Soc. Bull.*, 1997, **76**(12), 51–56.
4. Brown, A. S., Hypersonic designs with a sharp edge. *Aerospace Am.*, 1997, **35**(9), 20–21.
5. Norasetthekul, S., Eubank, P. T., Bradley, W. L., Bozkurt, B. and Stucker, B., Use of zirconium diboride–copper as an electrode in plasma applications. *J. Mater. Sci.*, 1999, **34**(6), 1261–1270.
6. Pastor, M., Metallic borides: preparation of solid bodies. sintering methods and properties of solid bodies. In *Boron and Refractory Borides*, ed. V. I. Matkovich. Springer, New York, 1977, pp. 457–493.
7. Monteverde, F. and Bellosi, A., Effect of the addition of silicon nitride on sintering behavior and microstructure of zirconium diboride. *Scripta Mater.*, 2002, **46**, 223–228.
8. Monteverde, F. and Bellosi, A., Development and characterization of metal-diboride-based composites toughened with ultra-fine sic particulates. *Solid State Sci.*, 2005, **7**, 622–630.
9. Monteverde, F. and Bellosi, A., Beneficial effects of AlN as sintering aid on microstructure and mechanical properties of hot-pressed ZrB_2. *Adv. Eng. Mater.*, 2003, **5**(7), 508–512.
10. Kuriakose, A. K. and Margrave, J. L., Oxidation kinetics of zirconium diboride and zirconium carbide at high temperatures. *J. Electrochem. Soc.*, 1964, **111**(7), 827–831.
11. Tripp, W. C., Davis, H. H. and Graham, H. C., Effect of an SiC addition on the oxidation of ZrB_2. *Am. Ceram. Soc. Bull.*, 1973, **52**(8), 612–616.
12. Rezaie, A., Fahrenholtz, W. G. and Hilmas, G. E., Oxidation of zirconium diboride–silicon carbide at 1500 °C at a low partial pressure of oxygen. *J. Am. Ceram. Soc.*, 2006, **89**(10), 3240–3245.

13. Sciti, D., Guicciardi, S., Bellosi, A. and Pezzotti, G., Properties of a pressureless-sintered ZrB_2–$MoSi_2$ ceramic composites. *J. Am. Ceram. Soc.*, 2006, **89**(7), 2320–2322.
14. Bellosi, A., Monteverde, F. and Sciti, D., Fast densification of ultra-high-temperature ceramics by spark plasma sintering. *Int. J. Appl. Ceram. Technol.*, 2006, **3**(1), 32–40.
15. Guo, S. Q., Nishimura, T., Kagawa, Y. and Tanaka, H., Thermal and electric properties in hot-pressed ZrB_2–$MoSi_2$–SiC composites. *J. Am. Ceram. Soc.*, 2007, **90**(7), 2255–2258.
16. Mendelson, M. I., Average grain size in polycrystalline ceramics. *J. Am. Ceram. Soc.*, 1969, **52**(8), 443–446.
17. Guo, S. Q., Hirosaki, N., Yamamoto, Y., Nishimura, T. and Mitomo, M., Hot-press sintering silicon nitride with Lu_2O_3 addition: elastic moduli and fracture toughness. *J. Eur. Ceram. Soc.*, 2003, **23**, 537–545.
18. Anstis, G. R., Chantikul, P., Lawn, B. R. and Marshall, D. B., A critical evaluation of indentation techniques for measuring fracture toughness. I. Direct crack measurements. *J. Am. Ceram. Soc.*, 1981, **64**(9), 533–538.
19. Monteverde, F., Guicciardi, S. and Bellosi, A., Advances in microstructure and mechanical properties of zirconium diboride based ceramics. *Mater. Sci. Eng. A*, 2003, **346**, 310–319.
20. Rezaie, A., Fahrenholtz, W. G. and Hilmas, G. E., Effect of hot-pressing time and temperature on the microstructure and mechanical properties of ZrB_2–SiC. *J. Mater. Sci.*, 2007, **42**, 2735–2744.
21. Zhu, S., Fahrenholtz, W. G. and Hilmas, G. E., Influence of silicon carbide particle size on the microstructure and mechanical properties of zirconium diboride-silicon carbide ceramics. *J. Eur. Ceram. Soc.*, 2007, **27**, 2077–2083.